Electronic Supplementary Material (ESI) for Journal of Materials Chemistry A.

Supporting Information for

# Preparation of porous $(Ni,Co)_3(BO_3)_2/Ni(OH)_2$ Nanosheet networks as pseudocapacitor materials with Superior Performance

Yuanzhen Chen[1,2], Yongning Liu[1*], Wei Yan[2*]

[1] State Key Laboratory for Mechanical Behavior of Materials, School of Material Science and Engineering, Xi'an Jiaotong University, Xi'an 710049, PR China

[2] School of Energy and Power Engineering, Xi'an Jiaotong University, Xi'an 710049, PR China

Corresponding authors:

Yong ning Liu , ynliu@mail.xjtu.edu.cn

Wei Yan, yanwei@mail.xjtu.edu.cn

Table S1. Ni and Co composited materials with large capacitance and good capacitance retention.

| Sample | Morphology | Capacitance ($F\cdot g^{-1}$) | Retention(%) | Ref. | Sample | Morphology | Capacitance ($F\cdot g^{-1}$) | Retention(%) | Ref. |
|---|---|---|---|---|---|---|---|---|---|
| **$CoMoO_4$/$NiMoO_4$ nanorods** | 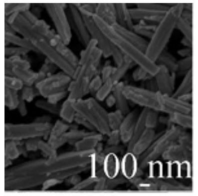 | 1039 ($2.5\ mA\cdot cm^{-1}$) | 72.3 ($100\ mA\cdot cm^{-1}$, 1000 cycles) | 1 | **$Co_3O_4$/$Ni(OH)_2$ nanosheets** | 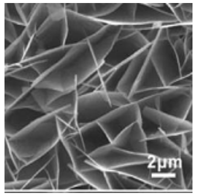 | 1144($5\ mV\cdot s^{-1}$) | 93.4 ($5\ mV\cdot s^{-1}$, 500 cycles) | 2 |
| **$Ni(OH)_2$/CoO/ graphene nanosheets** | 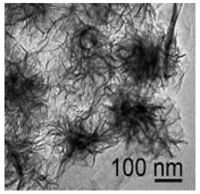 | 1056 ($5\ mV\cdot s^{-1}$) | 84.8 ($50mV\cdot s^{-1}$, 2000 cycles) | 3 | **doughnut-like $Ni(OH)_2$-$Co(OH)_2$** | 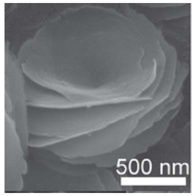 | 2020 ($5A\cdot g^{-1}$) | 84.7 ($5\ A\cdot g^{-1}$, 1000cycles) | 4 |
| **Ni–Co–O/ $Co_3O_4$ nanosheets** | 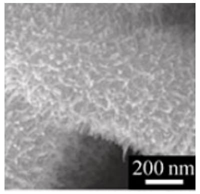 | 2098 ($5\ mA\cdot cm^{-1}$) | 96 ($30\ mA\cdot cm^{-2}$, 2000 cycles) | 5 | **Porous Nano-Ni/ $Co(OH)_2$ Nanoflake** | 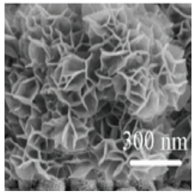 | 2028($5A\cdot g^{-1}$) | 95 ($2A\cdot g^{-1}$, 2000cycles) | 6 |
| **$Ni_3S_2$@$Ni(OH)_2$ / Graphene nanorods** | 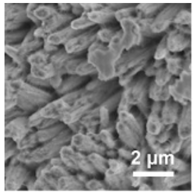 | 1125 ($5\ mV\cdot s^{-1}$),<br>1035 ($5.1\ A\cdot g^{-1}$) | 99.1 ($5.1A\cdot g^{-1}$, 2000 cycles) | 7 | **$Co_xNi_{1-x}(OH)_2$ nanoribbons** | 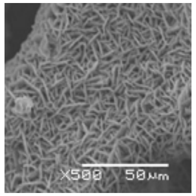 | 1200($4\ A\cdot g^{-1}$) | 86 ($1\ A\cdot g^{-1}$, 500cycles) | 8 |

1. Composite materials with a nanosheets morphology usually have large CPs.
2. Composite materials with a nanosheets morphology usually have good capacitance retention(>80% after 1000 cycles).

Table S2. comparison on specific surface area and capacitance for $Co_3O_4$ and other Ni/Co composites with different morphologies

| Sample | Morphology | SSA($m^2 \cdot g^{-1}$) | Capacitance ($F \cdot g^{-1}$) | Ref | Sample | Morphology | SSA($m^2 \cdot g^{-1}$) | Capacitance ($F \cdot g^{-1}$) | Ref |
|---|---|---|---|---|---|---|---|---|---|
| **$Co_3O_4$ nanorods** | 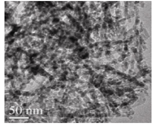 | 90.6 | 163 (2 $A \cdot g^{-1}$) | 9 | **$Ni(OH)_2$-$Co(OH)_2$ nanosheets** | 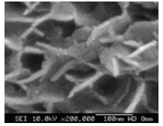 | 35.7 | 2104 (1 $A \cdot g^{-1}$) | 10 |
| **$Co_3O_4$ nanorods** | 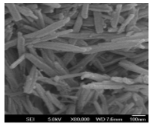 | 45.1 | 127.5 (1 $A \cdot g^{-1}$) | 11 | **Ni–Co–O/ $Co_3O_4$ nanosheets** | 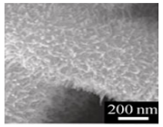 | 100 | 2098 (5 $mA \cdot cm^{-2}$) | 5 |
| **Mesopore $Co_3O_4$ big sheet** | 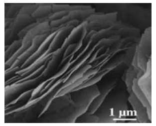 | 25.12 | 92 ( 5 $mA \cdot cm^{-2}$) | 12 | **Porous NiO nanospindles** | 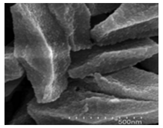 | 102.7 | 1462 (1 $A \cdot g^{-1}$) | 13 |
| **$Co_3O_4$ nanowires** | 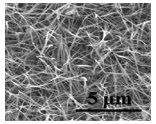 | 74.9 | 996 (1 $A \cdot g^{-1}$) | 14 | **$Co_{11}(HPO_3)_8(OH)_6$ nanoribbons** | 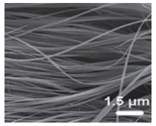 | 71.6 | 312 (1.25 $A \cdot g^{-1}$) | 15 |
| **$Co_3O_4$ nanowires** | 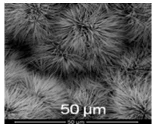 | 75.94 | 912 (0.25 $A \cdot g^{-1}$) | 16 | **NiO nanobelts** | 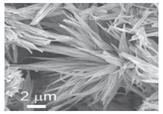 | 95.5 | 1126 (2 $A \cdot g^{-1}$) | 17 |
| **$Co_3O_4$ /NiO nanowires** | 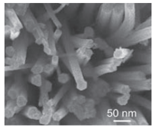 | 99.6 | 760(1 $A \cdot g^{-1}$) | 18 | **$Ni(OH)_2$ nanoplatelets** | 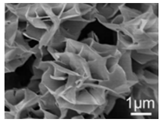 | 72.9 | 1750 (5 $mV \cdot s^{-1}$) | 19 |
| **$Co_3O_4$ nanosheets** | 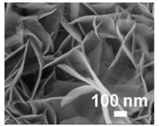 | 118 | 2735(2 $A \cdot g^{-1}$) | 20 | **$Co_3O_4$ /$Ni(OH)_2$ nanosheets** | 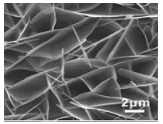 | 80.3 | 1144(5 $mV \cdot s^{-1}$) | 2 |

$Co_3O_4$ materials with different morphologies (nanorods, nanowires and nanosheets) had large gap in their specific capacitances (CPs), indicating that the morphology has a great influence on the redox process. Nanorods obtained low CPs, nanowires had high CPs, and nanosheets got higher CPs.

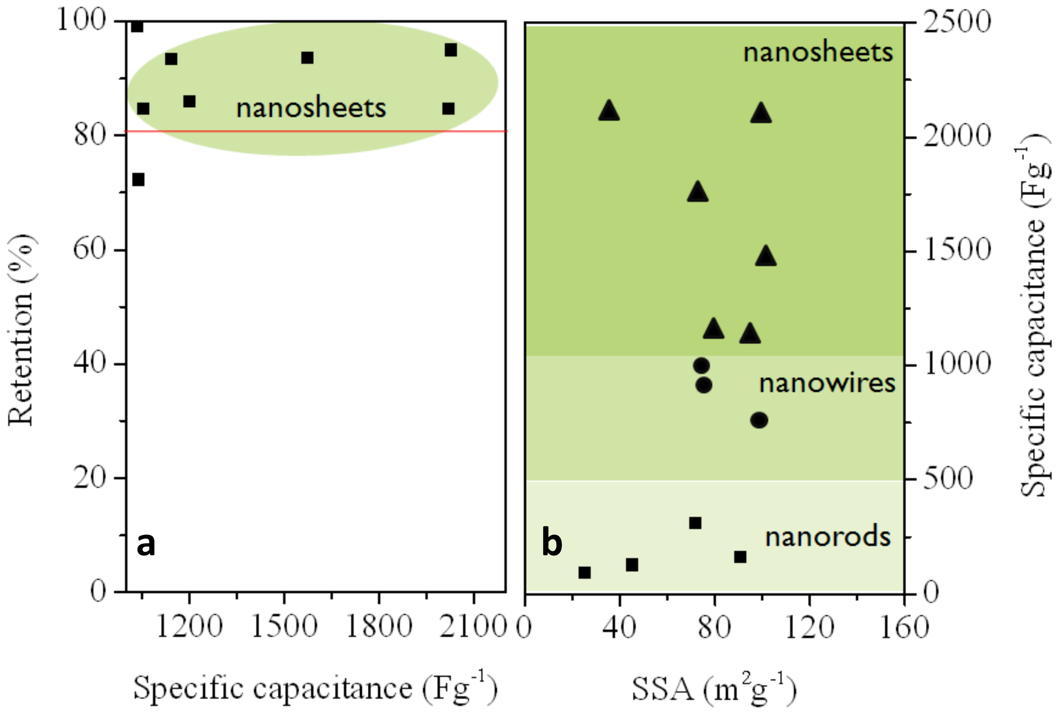

Figure S1. (a) Composite materials with a nanosheets morphology usually have large CPs and good capacitance retention (80% after 1000 cycles), driving from Table 2;(b) materials with different morphologies display large gap in specific capacitance, driving from Table 1.

The pure $Co_3(BO_3)_2$ and $Ni_3(BO_3)_2$ were prepared by the method mentioned by Gao et al,[21] and their SEM images, XRD patterns and CV curves are shown in **figure S2**. As seen from **figure S2 (a, b)**, $Ni_3(BO_3)_2$ and $Co_3(BO_3)_2$ show rodlike morphology which is different to the ultrathin nanosheets of $(Ni,Co)_3(BO_3)_2/Ni(OH)_2$ composite. XRD patterns (**figure S2. c**) determine that they are pure $Ni_3(BO_3)_2$ and $Co_3(BO_3)_2$. It is clearly seen that the pure Co3(BO3)2 and Ni3(BO3)2 have different redox peaks (**figure S2. d**). As seen from reduction peaks, $Co_3(BO_3)_2$ had four peaks and $Ni_3(BO_3)_2$ had two peaks respectively. Also compared with CV curve of Ni foam, it was clearly seen that the same peak located at 0.3 V should be the reduction peak of NiOOH[4]. Therefore, P1', P2' and P3' belonged to $Co_3(BO_3)_2$; P4' belonged to $Ni_3(BO_3)_2$. P1-P4 is the corresponding oxide peaks. The corresponding electrochemical reaction should be as follows:

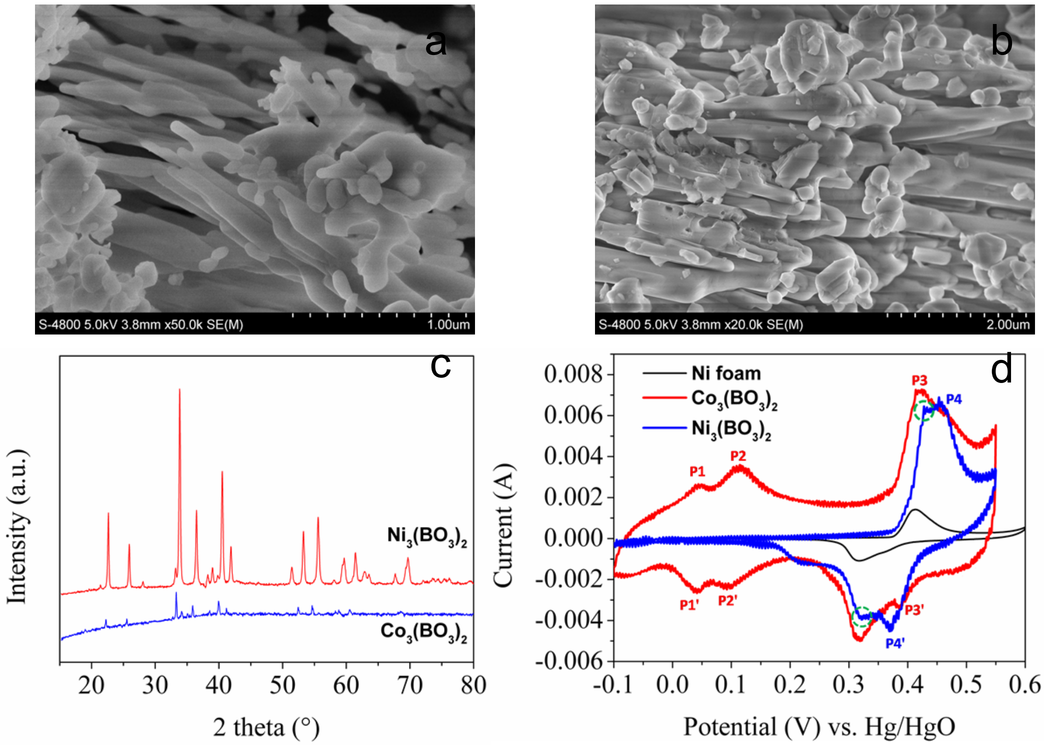

Figure S2. SEM images of (a) $Ni_3(BO_3)_2$ and (b) $Co_3(BO_3)_2$ prepared at 850 °C by the method mentioned by Gao et al.[21] (c) XRD patterns of $Ni_3(BO_3)_2$ and $Co_3(BO_3)_2$, (d) CV curves of $Ni_3(BO_3)_2$ and $Co_3(BO_3)_2$ measured at a scanning rate of 5 $mVs^{-1}$.

$$\frac{1}{2}Co_3(BO_3)_2 + OH^- \leftrightarrow \frac{1}{2}CoBO_3 + Co(OH)_2 + e^- \quad (P1 \leftrightarrow P1')$$

$$Co(OH)_2 + OH^- \leftrightarrow CoOOH + H_2O + e^- \quad (P2 \leftrightarrow P2')$$

$$CoOOH + OH^- \leftrightarrow CoO_2 + H_2O + e^- \quad (P3 \leftrightarrow P3')$$

$$\frac{1}{2}Ni_3(BO_3)_2 + OH^- \leftrightarrow NiBO_3 + \frac{1}{2}Ni(OH)_2 + e^- \quad (P4 \leftrightarrow P4')$$

Specially, for $Co_3(BO_3)_2$ sample, the oxidation peak corresponding to P3' overlaps the oxidation peak of Ni foam, because the reduction peaks at 0.4V (P3') and 0.3V separate from each other. For $Ni_3(BO_3)_2$ sample, it has two reduction peaks at 0.375V (P4') and 0.3V(green circle). Correspondingly, there are two oxidation peaks 0.43 V (green circle) and 0.45 V (P4). The redox peaks marked by green circle should belong to Ni foam. The redox peaks (P4-P4') belong to $Ni_3(BO_3)_2$. Even though the electrochemical oxidation products of $Ni_3(BO_3)_2$ include $Ni(OH)_2$, the oxidation potential of

$Ni_3(BO_3)_2$ is higher than that of $Ni(OH)_2$, therefore, when potential exceeds 0.45 V (P4), no one oxidation peak of $Ni(OH)_2$ appears.

However, the CV curve of $(Ni,Co)_3(BO_3)_2/Ni(OH)_2$ composite as positive electrode material (**figure 4.c in text**) only shows one pair of broad peaks, and one weak reduction peak (arrow in figure 4.c ) which should belong to $Ni(OH)_2$. The electrochemical reaction of $Ni(OH)_2$ is:

$$Ni(OH)_2 + OH^- = NiOOH + H_2O + e^-$$

Other clear peaks appeared in **figure S2.d** maybe overlap each other and then display in broad oxidation and reduction peaks.

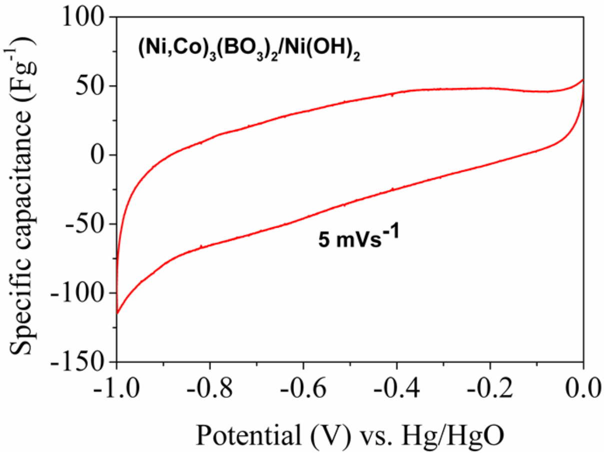

Figure S3. The CV curve of $(Ni,Co)_3(BO_3)_2/Ni(OH)_2$ composite as negative electrode at a scanning rate of 5 $mVs^{-1}$.

## References

1 M.-C. Liu, L.-B. Kong, C. Lu, X.-J. Ma, X.-M. Li, Y.-C. Luo and L. Kang, *J. Mater. Chem. A*, 2013, **1**, 1380.

2 J.-H. Zhong, A.-L. Wang, G.-R. Li, J.-W. Wang, Y.-N. Ou and Y.-X. Tong, *J. Mater. Chem.*, 2012, **22**, 5656.

3 L. Jiang, R. Zou, W. Li, J. Sun, X. Hu, Y. Xue, G. He and J. Hu, *J. Mater. Chem. A*, 2013, **1**, 478.

4 J. Li, M. Yang, J. Wei and Z. Zhou, *Nanoscale*, 2012, **4**, 4498.

5 Z. Lu, Q. Yang, W. Zhu, Z. Chang, J. Liu, X. Sun, D. Evans and X. Duan, *Nano Res.*, 2012, **5**, 369.

6 X. H. Xia, J. P. Tu, Y. Q. Zhang, Y. J. Mai, X. L. Wang, C. D. Gu and X. B. Zhao, *J. Phys. Chem. C*, 2011, **115**, 22662.

7 W. Zhou, X. Cao, Z. Zeng, W. Shi, Y. Zhu, Q. Yan, H. Liu, J. Wang and H. Zhang, *Energy Environ. Sci.*, 2013, **6**, 2216.

8 X. Liu, J. Huang, X. Wei, C. Yuan, T. Liu, D. Cao, J. Yin and G. Wang, *J. Power Sources*, 2013, **240**, 338.

9 Y. Wang, Z. Zhong, Y. Chen, C. Ng and J. Lin, *Nano Res.*, 2011, **4**, 695.

10 V. Gupta, S. Gupta and N. Miura, *J. Power Sources*, 2008, **175**, 680.

11 D. Wang, Q. Wang and T. Wang, *Inorg. Chem.*, 2011, **50**, 6482.

12 S. Xiong, C. Yuan, X. Zhang, B. Xi and Y. Qian, *Chem.-Eur. J.* 2009, **15**, 5320.

13 H. Pang, B. Zhang, J. Du, J. Chen, J. Zhang and S. Li, *RSC Adv.*, 2012, **2**, 2257.

14 F. Zhang, C. Yuan, X. Lu, L. Zhang, Q. Che and X. Zhang, *J. Power Sources*, 2012, **203**, 250.

15 H. Pang, Y. Liu, J. Li, Y. Ma, G. Li, Y. Ai, J. Chen, J. Zhang and H. Zheng, *Nanoscale*, 2013, **5**, 503.

16 R. B. Rakhi, W. Chen, D. Cha and H. N. Alshareef, *Nano Lett.*, 2012, **12**, 2559.

17 B. Wang, J. S. Chen, Z. Wang, S. Madhavi and X. W. Lou, *Adv. Energy Mater.*, 2012, **2**, 1188.

18 H. Wang, Q. Gao and L. Jiang, *Small*, 2011, **7**, 2454.

19 H. Jiang, T. Zhao, C. Li and J. Ma, *J. Mater. Chem.*, 2011, **21**, 3818.

20 C. Yuan, L. Yang, L. Hou, L. Shen, X. Zhang and X. W. Lou, *Energy Environ. Sci.*, 2012, **5**, 7883.

21 H. Pang, Q. Lu, C. Chen, X. Liu and F. Gao, *J. Mater. Chem.*, 2011, **21**, 13889.